Coenzyme A-Disulfide Reductase from *Staphylococcus aureus*: Evidence for Asymmetric Behavior on Interaction with Pyridine Nucleotides†

James Luba,‡ Véronique Charrier,‡ and Al Claiborne*

Department of Biochemistry, Wake Forest University Medical Center, Winston-Salem, North Carolina 27157

Received October 30, 1998; Revised Manuscript Received December 21, 1998

ABSTRACT: An unusual flavoprotein disulfide reductase, which catalyzes the NADPH-dependent reduction of CoASSCoA, has recently been purified from the human pathogen *Staphylococcus aureus* [delCardayré, S. B., Stock, K. P., Newton, G. L., Fahey, R. C., and Davies, J. E. (1998) *J. Biol. Chem. 273*, 5744−5751]. Coenzyme A-disulfide reductase (CoADR) lacks the redox-active protein disulfide characteristic of the disulfide reductases; instead, NADPH reduction yields 1 protein-SH and 1 CoASH. Furthermore, the CoADR sequence reveals the presence of a single putative active-site Cys (Cys43) within an SFXXC motif also seen in the *Enterococcus faecalis* NADH oxidase and NADH peroxidase, which use a single redox-active cysteine-sulfenic acid in catalysis. In this report, we provide a detailed examination of the equilibrium properties of both wild-type and C43S CoADRs, focusing on the role of Cys43 in the catalytic redox cycle, the behavior of both enzyme forms on reduction with dithionite and NADPH, and the interaction of $NADP^+$ with the corresponding reduced enzyme species. The results of these analyses, combined with electrospray mass spectrometric data for the two oxidized enzyme forms, fully support the catalytic redox role proposed for Cys43 and confirm that this is the attachment site for bound CoASH. In addition, we provide evidence indicating dramatic thermodynamic inequivalence between the two active sites per dimer, similar to that documented for the related enzymes mercuric reductase and NADH oxidase; only 1 FAD is reduced with NADPH in wild-type CoADR. The EH_2·NADPH/EH_4·$NADP^+$ complex which results is reoxidized quantitatively in titrations with CoASSCoA, supporting a possible role for the asymmetric reduced dimer in catalysis.

The pyridine nucleotide-disulfide oxidoreductases have been described as a family of (mostly) homodimeric flavoenzymes containing one redox-active disulfide and one FAD per monomer (*1*). While the NADH oxidase (Nox)[1] and NADH peroxidase (Npx) from *Enterococcus faecalis* contain cysteine-sulfenic acid (Cys-SOH) redox centers instead of redox-active disulfides and catalyze electron transfers between NADH and O_2 or H_2O_2 instead of disulfide substrates (*2*−*4*), structural analyses make it abundantly clear that these two unusual flavoproteins should be considered as members of the disulfide reductase family (*5*, *6*). More specifically, Nox and Npx have been compared with that class of disulfide reductases represented by glutathione reductase (GR; *7*); GR is widely distributed among aerobic organisms and functions to maintain a high intracellular GSH/GSSG ratio, by virtue of the NADPH-dependent reduction of GSSG which it catalyzes. The mechanism of GSSG reduction involves distinct roles for each of the nascent protein thiols generated from the active-site disulfide, and the fact that Nox and Npx function catalytically with only one active-site Cys-SH in the respective reduced enzyme form provides a fundamental mechanistic contrast with the GR-like enzymes (*1*, *8*).

Several examples of flavoprotein disulfide reductases, functionally similar to GR but with different disulfide substrate specificities, have been purified from Gram-positive Eubacteria and Archaea; these include the pantethine 4′,4″-diphosphate reductase from *Bacillus megaterium* (*9*) and the coenzyme M-disulfide reductase from *Methanobacterium thermoautotrophicum* ΔH (*10*). Recently, delCardayré et al. have purified and characterized a coenzyme A-disulfide reductase (CoADR) from the Gram-positive human pathogen *Staphylococcus aureus* (*11*); sequence analysis of the *cdr* gene revealed (*12*), quite surprisingly, the absence of any redox-active disulfide motif. Instead, 1 of the 2 Cys residues/CoADR subunit (Cys43) was found within a conserved active-site sequence (SFXXC) that is attributed to Nox and Npx. Reduction of the enzyme with NADPH led to the release of 1 CoASH/subunit and generated 1 DTNB-reactive protein-SH not present in the oxidized enzyme; a stable Cys43-SSCoA mixed disulfide structure was proposed for the oxidized form of the non-flavin redox

† This work was supported by National Institutes of Health Grant GM-35394.

* To whom correspondence should be addressed: Department of Biochemistry, Wake Forest University Medical Center, Medical Center Boulevard, Winston-Salem, NC 27157. Telephone: (336) 716-3914. Fax: (336) 716-7671. URL: http://invader.bgsm.wfu.edu/.

‡ These authors contributed equally to this work.

[1] Abbreviations: Nox, NADH oxidase; Npx, NADH peroxidase; Cys-SOH, cysteine-sulfenic acid; GR, glutathione reductase; CoADR, coenzyme A-disulfide reductase; DTNB, 5,5′-dithiobis(2-nitrobenzoic acid); IPTG, isopropyl β-D-thiogalactopyranoside; TB, Terrific Broth; CoAD, coenzyme A-disulfide; HEPES, *N*-(2-hydroxyethyl)piperazine-*N*′-(2-ethanesulfonic acid); ESI-MS, electrospray interface-mass spectrometry; EH_2, two-electron reduced enzyme (FAD, Cys-SH); EH_4, four-electron reduced enzyme ($FADH_2$, Cys-SH); LipDH, lipoamide dehydrogenase; E'°, midpoint oxidation−reduction potential at pH 7.0; E, oxidized enzyme; EH'_2, two-electron reduced enzyme ($FADH_2$, −SX); MR, mercuric reductase.

10.1021/bi9825899 CCC: $18.00
Published on Web 02/09/1999

center. The enzyme also contained 1 FAD/subunit, and the recombinant CoADR as expressed and purified from *Escherichia coli* was shown to be functionally identical to the enzyme purified from *S. aureus.*

To further examine the essential catalytic role proposed for Cys43, we present in this report a detailed analysis of the equilibrium properties of wild-type and C43S mutant CoADRs, focusing on static titrations designed to allow a quantitative description of the redox and $NADP^+$-binding behavior of both enzyme forms. These results indicate quite clearly that wild-type CoADR, like Nox (*2*, *3*), exhibits strong active-site asymmetry on reduction with the pyridine nucleotide substrate.

EXPERIMENTAL PROCEDURES

Materials. NADPH, $NADP^+$, and NADH were purchased from Boehringer Mannheim, and adenosine 2,5-diphosphate agarose was from Sigma. CoAD was purchased from Fluka, and potassium ferricyanide was from Fisher. IPTG was purchased from Ambion; DTNB was from Aldrich, and ultrapure urea was from ICN. All other chemicals and restriction enzymes, as purchased from sources described previously (*3*, *13*), were of the best grades available.

Expression and Purification of Wild-Type and C43S CoADRs. The pXCDR expression plasmid containing the wild-type *cdr* gene (*12*) was generously provided by S. delCardayré and J. Davies. The *Xba*I−*Eco*RI fragment encoding the 315 N-terminal residues was subcloned into pBluescript II KS(+) and used as a template for Cys43 → Ser mutagenesis, using the Sculptor kit (Amersham). After the presence of this single mutation was confirmed, the *Xba*I−*Eco*RI fragment was used to replace the corresponding wild-type segment in pXCDR. Recombinant wild-type (and C43S) CoADR was expressed and purified following an adaptation of the general protocol described by delCardayré et al. (*11*, *12*). *E. coli* BL21(DE3) transformed with either pXCDR or pC43S was grown in ten 2.8 L Fernbach flasks, each containing 0.6 L of TB medium with 0.4 mg/mL ampicillin. Flasks were shaken vigorously at 37 °C until the cultures reached an A_{600} of 1.0, and 1 mM IPTG was added at that time. After induction for 3 h, cells were harvested by centrifugation; the pellet was resuspended in 20 mM Tris-HCl (pH 7.4, as measured at 25 °C), and 1 mM EDTA, and disrupted by passage through an SLM/Aminco French press. After centrifugation, the crude extract was brought to 50% saturation (as defined at 25 °C) with solid ammonium sulfate. The resulting supernatant was then brought to 80% saturation with ammonium sulfate; the resulting protein pellet was resuspended in a minimal volume of Tris-EDTA buffer and dialyzed twice against 4 L of this buffer. The dialyzed protein was applied to a 10 mL column of adenosine 2,5-diphosphate agarose equilibrated with the same buffer. After the column was washed, the enzyme was eluted with a 0 to 4 M NaCl gradient, and fractions with an A_{280}/A_{452} of <9 (A_{280}/A_{444} < 7 for C43S CoADR) were pooled and buffer-exchanged by ultrafiltration into 50 mM potassium phosphate (pH 7.0) and 0.5 mM EDTA. The pure enzyme was then concentrated to 10 mg/mL in the same buffer with 20% (v/v) glycerol before being stored at −80 °C.

General Procedures. CoADR activity was assayed at 25 °C in a total volume of 3 mL containing 50 mM potassium phosphate (pH 7.0), 0.5 mM EDTA, 32 μM NADPH, and 60 μM CoAD. One unit of activity is defined as the amount of enzyme catalyzing the oxidation of 1 μmol of NADPH (decrease in A_{340}) per minute at 25 °C. Anaerobic titrations and DTNB assays followed established protocols (*3*, *14*), using Hewlett-Packard model 8452A and Beckman DU 7500 spectrophotometers and an SLM Aminco-Bowman Series 2 spectrofluorimeter. The ENZFITTER (*15*) program was used to analyze the binding of $NADP^+$ to reduced C43S CoADR. The extinction coefficients used have previously been reported (in M^{-1} cm^{-1}): NADPH, 6200 at 340 nm (*16*); $NADP^+$, 18 000 at 260 nm; NADH, 6220 at 340 nm; CoAD, 33 600 at 260 nm (*11*); $K_3Fe(CN)_6$, 1000 at 420 nm (*17*); 5-thio-2-nitrobenzoate, 13 700 at 412 nm (*14*); and wild-type CoADR, 12 800 at 452 nm (*11*). An ϵ_{260} value of 16 400 M^{-1} cm^{-1} (*16*) was used for $AcPyADP^+$, and the ϵ_{444} value for C43S CoADR was determined as described earlier for Npx (*18*).

ESI-MS analyses were provided by the Analytical Chemistry Core Laboratory (Comprehensive Cancer Center of Wake Forest University), following established protocols (*19*).

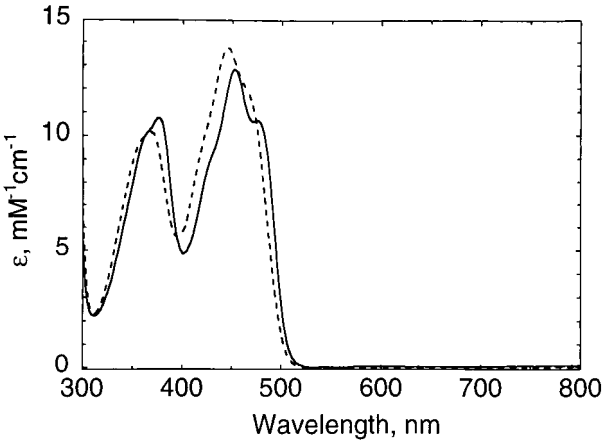

FIGURE 1: Comparison of the visible absorption spectrum of oxidized wild-type CoADR (—) with that of the C43S mutant enzyme (- - -). Spectra were recorded for the proteins in 50 mM phosphate buffer (pH 7.0) and 0.5 mM EDTA at 23 °C.

RESULTS

Spectral and Catalytic Properties of Wild-Type and C43S CoADRs. Protocols for expression and purification of wild-type and C43S CoADRs closely followed the procedures described by delCardayré et al. (*11*, *12*), with modifications as noted in Experimental Procedures. The average yield for each of the two proteins was about 190 mg from 6 L of recombinant *E. coli*, representing a significant improvement over that originally reported (5−10 mg/L; *12*). Figure 1 gives the visible absorption spectra of the recombinant wild-type CoADR (λ_{max} = 376 and 452 nm, ϵ_{452} = 12 800 M^{-1} cm^{-1}) and the C43S mutant (λ_{max} = 366 and 444 nm, ϵ_{444} = 13 700 M^{-1} cm^{-1}). The wild-type spectrum also exhibits a strong shoulder at 478 nm as previously noted (*11*), and the hyperchromic blue shift in the absorbance maximum of the mutant is similar to those observed when Cys42 in the closely related Nox (*2*) and Npx (*20*), respectively, is replaced by Ser. The absorbance ratios at 280 and 450 nm for wild-type and mutant CoADRs are 7.1 and 5.9; the value for the wild-

type enzyme is comparable to that of about 6.7 reported for the enzyme as purified from *S. aureus* (*11*). Both forms of CoADR exhibit diminished flavin fluorescence, with quantum yields that are about 7 and 12% of that of free FAD for the wild-type and C43S mutant proteins, respectively. The C42S mutants of Nox and Npx have quantum yields of 37 (*2*) and 18% (*20*), respectively, relative to free FAD.

delCardayré et al. (*11*), using a direct spectrophotometric assay for CoAD-dependent NADPH oxidation at 37 °C, reported a k_{cat} of 1000 s^{-1} and a K_m(CoAD) of 11 μM ($k_{cat}/K_m = 9.1 \times 10^7$ M^{-1} s^{-1}) in a standard buffer of 50 mM Tris-HCl (pH 7.8) containing 50 mM NaCl. At 37 °C, this would correspond to a specific activity of about 1200 units/mg, using a subunit molecular weight of 50 711 (including FAD and CoASH) for CoADR. Using the stopped-flow spectrophotometer to obtain highly reproducible initial velocity measurements at 340 nm (*21*), with final NADPH and CoAD concentrations of 0.1 mM each, we evaluated the pH, buffer, and NaCl dependence for recombinant wild-type enzyme activity (final [CoADR] = 0.1 μM) from pH 7.0 to 8.0 at 25 °C. With potassium phosphate, HEPES, and Tris-sulfate buffers, we observed a pH optimum from pH 7.0 to 7.5 that corresponded to a specific activity of 34 units/mg in 0.1 M phosphate and 0.5 mM EDTA. The presence of EDTA concentrations as high as 10 mM has previously been reported to have no effect on the kinetics observed for CoADR (*11*). Activity in 50 mM Tris-sulfate (pH 7.5) was virtually identical to that in 0.1 M phosphate; in both buffers, the presence of NaCl had either slight or moderate inhibitory effects. On the basis of these and other analyses, we decided to select a standard assay buffer of 50 mM potassium phosphate (pH 7.0) and 0.5 mM EDTA, with 32 μM NADPH and 60 μM CoAD. The specific activity of 34 units/mg corresponds to a turnover number of about 29 s^{-1} at 25 °C; a thorough steady-state analysis has been completed which gives a k_{cat} of 27 s^{-1} with a K_m(NADPH) of 0.2 μM and a K_m(CoAD) of 3 μM. A detailed study of the kinetic mechanism, including stopped-flow analyses of the NADPH and CoAD reactions, is in progress and will be described in a separate communication.[2]

The specific activity for several preparations of wild-type CoADR ranged from 29 to 34 units/mg ($k_{cat} = 25-29$ s^{-1}), and the activity with 0.1 mM NADH replacing NADPH corresponds to a k_{cat} of about 4−5 s^{-1}. NADPH oxidase and NADPH-dependent glutathione reductase (2.25 mM GSSG replacing CoAD) activities were both <1% of the CoADR activity. The C43S mutant catalyzes a similar weak NADPH oxidase activity; after correcting for this background NADPH oxidation in the standard CoADR assay, the C43S enzyme has only about 0.03% activity relative to wild-type CoADR. This result is fully consistent with the proposal of delCardayré et al. (*11*) in which Cys43-SH serves as the essential nucleophile in the thiol−disulfide interchange catalyzed by CoADR; it also adds further support to the conclusion (*12*) that CoADR should be considered a third member of that flavoprotein disulfide reductase group represented by Nox and Npx.

Electrospray Mass Spectrometric Analysis. delCardayré et al. (*11*) have shown that NADPH reduction of CoADR gives two DTNB-reactive protein thiols (as assayed in 4 M urea) and one low-molecular weight thiol which was identified as CoASH. Since CoADR samples assayed for DTNB-reactive thiols without prior NADPH reduction give only one protein-SH per subunit (attributed to Cys16; *12*), there is 1 equiv of CoASH bound per Cys43 in the enzyme as purified from either source. Therefore, the C43S mutant, as analyzed by ESI-MS, should give a subunit mass reflecting both the Cys → Ser mutation (−15 Da) and the loss of bound CoASH (−767 Da). Since the noncovalently bound FAD dissociates in the acidic solvent (0.1% formic acid in 50% acetonitrile) employed in sample preparation, and since the N-terminal Met is cleaved in both *S. aureus* and *E. coli* (*12*), the calculated mass for the C43S mutant is 49 143 Da. As shown in Figure 2, the observed mass is 49 145 Da (±5 Da), confirming that Cys43 in wild-type CoADR is the attachment site for CoASH. In addition, the excellent agreement with the mass predicted from the *cdr* gene sequence demonstrates that there are no unanticipated substitutions or mutations which could give rise to the differences observed in wild-type enzyme activities, as described above. The calculated mass for wild-type CoADR (including 1 equiv of CoASH) is 49 926 Da. The spectrum given in Figure 2 is clearly indicative of microheterogeneity in the sample; this is seen for different preparations and appears to be independent of long-term storage of the protein at −80 °C. The transformed spectrum gives two *m* values of 49 965 and 49 921 Da; the second value is in excellent agreement with the calculated mass, but the first component represents an increase of 39 Da. The absence of similar heterogeneity in the C43S protein suggested that the CoASH moiety or the Cys43-SSCoA mixed disulfide was the source of this difference; this suggestion was tested further by analyzing the protein after incubation with NADPH, as described by delCardayré et al. (*11*). Although subsequent ESI-MS analysis demonstrated the presence of a significant level of residual oxidized CoADR ($m = 49\,923$ Da), the major peak now corresponds to a mass of 49 153 Da, in very good agreement with the value of 49 159 Da calculated for reduced (without CoASH) CoADR. The reduced component also lacks the microheterogeneity observed in the oxidized enzyme, further pointing to the bound CoASH moiety as the source of the +39 Da difference. At present, the chemical basis for this difference

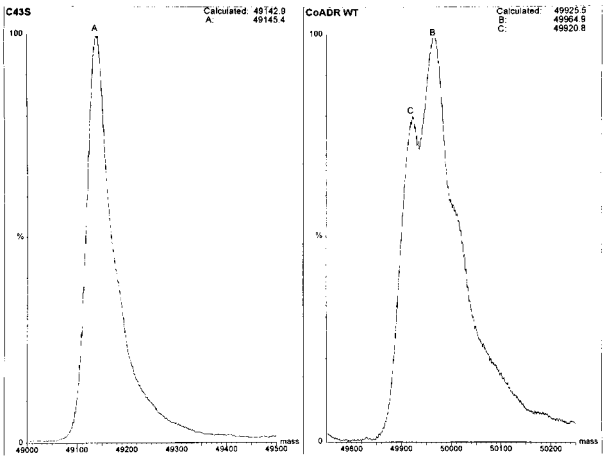

FIGURE 2: Transformed electrospray mass spectra of C43S (left) and wild-type (right) CoADRs. The deconvoluted mass value for C43S is 49 145 Da; the wild-type enzyme gives at least two major components of 49 921 and 49 965 Da.

[2] J. Luba and A. Claiborne, unpublished results.

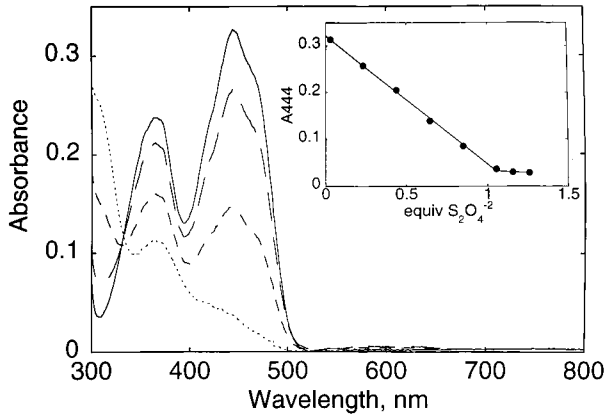

FIGURE 3: Anaerobic titration of C43S CoADR with dithionite. The anaerobic cuvette contained 0.75 mL of 24.7 μM enzyme (FAD) in the phosphate/EDTA buffer (pH 7.0). Spectra shown in order of decreasing A_{444} correspond to oxidized enzyme (—) and enzyme after addition of 0.24 (— —), 0.65 (— —), and 1.18 (- -) equiv of dithionite/FAD. In the inset is depicted the absorbance change at 444 nm vs the number of equivalents of dithionite added. The end point corresponds to 1.1 equiv of dithionite/FAD.

remains unknown [tightly bound potassium ion (K^+, 39 Da) is one possibility], but it does not appear to involve the CoADR polypeptide per se.

Titrations of C43S and Wild-Type CoADRs with Dithionite. The demonstration that NADPH reduction of wild-type CoADR generates one new protein-SH and one free CoASH, in conjunction with the ESI-MS data presented above and the virtual absence of CoADR activity in the C43S mutant, supports the existence of a redox-active Cys43-SSCoA mixed disulfide in the oxidized enzyme. Dithionite titration of the wild-type enzyme should therefore require 2 equiv of reductant per FAD, but the C43S mutant should require only 1 equiv of dithionite for complete reduction. Figure 3 gives the result of such a titration with the mutant; direct reduction of the flavin is observed with 1.1 equiv of dithionite, as expected. Virtually no flavin semiquinone appears; this titration clearly demonstrates the absence of any non-flavin redox center in the mutant. In addition to the 2 equiv of dithionite per FAD reduction stoichiometry expected for wild-type CoADR, the EH_2 forms of all GR-like disulfide reductases exhibit significant Cys-S^- → FAD charge-transfer absorbance between 510 and 550 nm (*1*). We therefore expected addition of 1 equiv of dithionite per wild-type CoADR subunit to yield such a charge-transfer intermediate. However, as shown in Figure 4A, the only long-wavelength absorbance observed can be attributed to a modest extent of neutral flavin semiquinone stabilization, not seen with the C43S mutant. The first phase of the titration, monitored at 452 nm, consists of a lag equivalent to addition of 1 mol of dithionite/FAD; this is consistent with preferential reduction of a non-flavin redox center, i.e., the Cys43-SSCoA disulfide. The nascent Cys43-SH does not appear to interact with FAD as a charge-transfer donor, however. Addition of a second equivalent of dithionite/FAD leads directly to the fully reduced EH_4 form of CoADR.

Although the fluorescence quantum yield of the wild-type enzyme is <10% of that of free FAD, subsequent analysis of the fluorescence change accompanying the dithionite titration indicated that 90% of the fluorescence (λ^{EX} = 452 nm, λ^{EM} = 520 nm) was lost during the first phase of

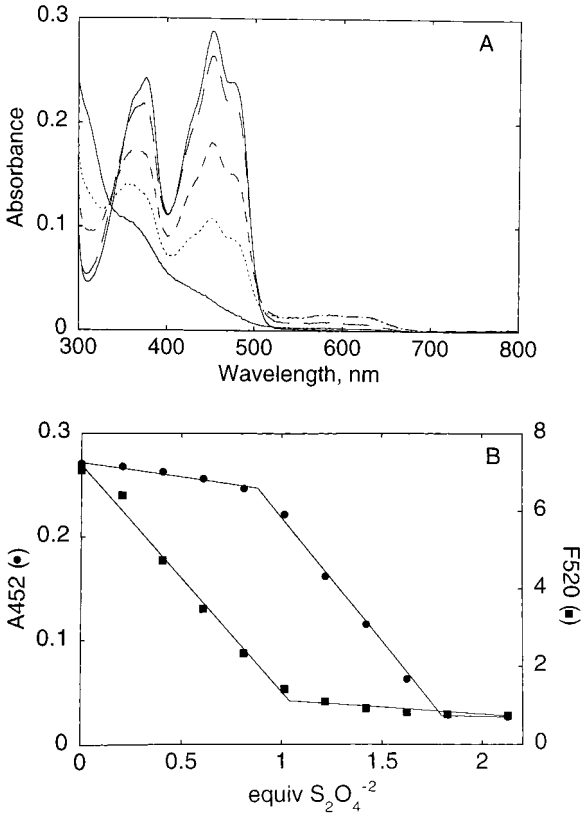

FIGURE 4: Anaerobic titration of wild-type CoADR with dithionite. (A) The 22.4 μM enzyme (0.75 mL) in phosphate/EDTA buffer (pH 7.0) was reduced; spectra shown in order of decreasing A_{452} correspond to oxidized enzyme (—) and enzyme after addition of 0.7 (— —), 1.15 (— —), 1.45 (- -), and 1.98 (—) equiv of dithionite/FAD. (B) Changes in absorbance at 452 nm and FAD fluorescence (λ^{EX} = 452 nm, λ^{EM} = 520 nm) vs the number of equivalents of dithionite added. These data were obtained in an experiment similar to that described in panel A, but with 8.7 μM CoADR. The respective end points are 0.9 and 1.8 equiv (A_{452}) and 1.05 equiv (F_{520}) of dithionite/FAD.

reduction. The plot of F_{520} versus the number of equivalents of dithionite given in Figure 4B yields an end point of 1.05 mol of reductant/FAD, while the A_{452} data for the same titration show clearly that full reduction requires 1.78 equiv/FAD. These data are consistent with the following redox scheme for wild-type CoADR:

Scheme 1

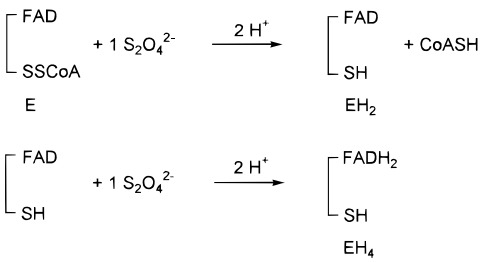

Although the EH_2 form does not exhibit Cys43-S^- → FAD charge-transfer absorbance, the fluorescence of this species is largely quenched relative to that of the oxidized enzyme; the nascent Cys43-SH could play a direct role in this quenching.

Reductive Titrations with NADPH. As expected on the basis of the dithionite titration described above, NADPH

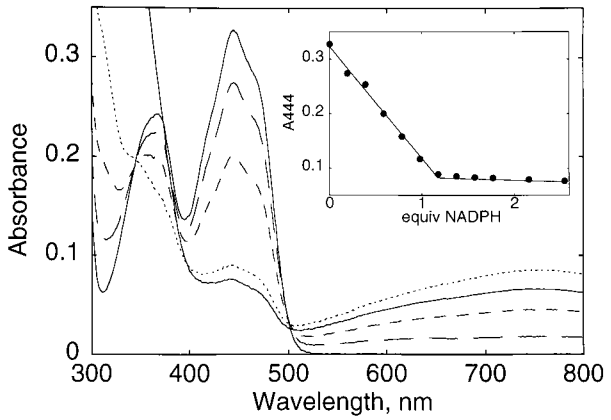

FIGURE 5: Anaerobic titration of C43S CoADR with NADPH. The 23.3 μM enzyme (0.79 mL) was reduced in the phosphate/EDTA buffer; spectra shown in order of decreasing A_{444} correspond to oxidized enzyme (—) and enzyme after addition of 0.2 (— —), 0.6 (— —), 1.2 (- -), and 2.9 (—) equiv of NADPH/FAD. In the inset is depicted the absorbance change at 444 nm vs the number of equivalents of NADPH added. The end point corresponds to 1.15 equiv of NADPH/FAD. The oxygen-scrubbing system consisting of protocatechuate dioxygenase and protocatechuic acid was added anaerobically prior to the titration.

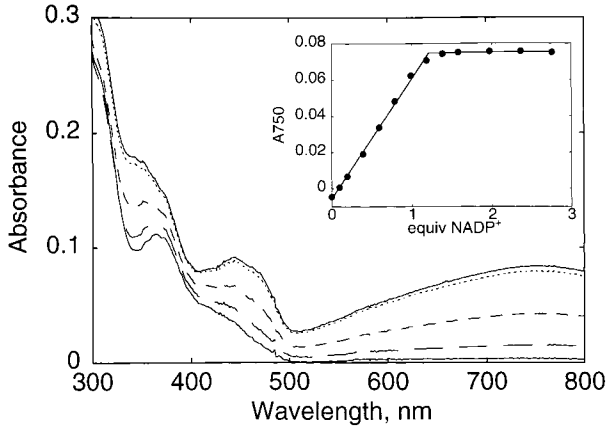

FIGURE 6: $NADP^+$ titration of reduced C43S CoADR. The 24.7 μM enzyme (0.75 mL) was reduced with 1.4 equiv of dithionite/FAD in the phosphate/EDTA buffer. After the dithionite syringe was exchanged for one containing 2.75 mM $NADP^+$, the titration was continued; spectra shown in order of increasing A_{700} correspond to the reduced enzyme (—) and reduced enzyme after the addition of 0.2 (— —), 0.6 (— —), 1.18 (- -), and 1.58 (—) equiv of $NADP^+$/FAD. In the inset is depicted the absorbance change at 750 nm vs the number of equivalents of $NADP^+$ added. The end point corresponds to 1.2 equiv of $NADP^+$/FAD.

reduction of C43S CoADR (Figure 5) requires 1.15 equiv of reductant/FAD; the formation of the resulting $E-FADH_2 \cdot NADP^+$ charge-transfer complex is observed at 750 nm. On addition of a small excess of NADPH (total of 2.53 equiv/FAD), however, there are secondary spectral changes which lead to a further decrease in A_{444} as well as loss of about 20% of the charge-transfer absorbance. In a very similar experiment where flavin absorbance and fluorescence ($\lambda^{EX} = 450$ nm, $\lambda^{EM} = 510$ nm), as well as NADPH fluorescence, were monitored, it was clearly demonstrated that the A_{444} and F_{510} end points were identical. Similarly, the NADPH fluorescence analysis ($\lambda^{EX} = 340$ nm, $\lambda^{EM} = 470$ nm) demonstrated quantitative quenching of pyridine nucleotide fluorescence with an end point of 1.08 equiv/FAD. The most likely explanation for the secondary changes in the $E-FADH_2 \cdot NADP^+$ absorbance spectrum would involve partial displacement of the bound $NADP^+$ in the presence of excess NADPH. We furthermore demonstrated that $NADP^+$ titration of dithionite-reduced C43S CoADR (Figure 6) gave the same charge-transfer complex as observed in the forward NADPH titration; $NADP^+$ binding does induce a significant increase in A_{444}, as well as the characteristic increase in A_{750}. All spectral changes are fully saturable on addition of 1.1−1.2 equiv of $NADP^+/FADH_2$, and there is absolutely no evidence for any $FADH_2 \rightarrow NADP^+$ electron-transfer component; nor is any $NADP^+$-sulfite adduct formation observed as was recently reported in similar titrations of C42S NADH oxidase (*2*). The $K_d(NADP^+)$ estimated from a direct plot of ΔA_{750} versus the number of equivalents of $NADP^+$ per $FADH_2$ is ≤ 1 μM, suggesting that NADPH must be able to bind the reduced C43S mutant with an apparent K_d in the 50 μM range.

NADPH titration of wild-type CoADR (Figure 7A) follows a course that is dramatically different, as expected, from reduction of the mutant. Two distinct phases can be monitored at several wavelengths, corresponding to overall end points from 1.72 to 1.81 equiv of NADPH/FAD. In addition, it appears that only 1 FAD/dimer is reduced by NADPH, as the A_{452} minimum reached at 1 equiv of NADPH/FAD still corresponds to 60% of the starting oxidized CoADR absorbance. The first phase of the titration requires 0.9−1.05 equiv of NADPH (Figure 7B) as determined at 452, 505 (data not shown), and 750 nm; there is an isosbestic point at 503 nm as reduction of 1 FAD/dimer proceeds with the appearance of the $E-FADH_2 \cdot NADP^+$ complex. In sharp contrast to the dithionite titration, there is no lag corresponding to a distinct stage of Cys43-SSCoA reduction. Furthermore, since only 1 FAD is reduced in this first phase requiring 2 equiv of NADPH/dimer, it appears that 1 Cys43-SSCoA disulfide (per dimer) is also reduced. As in the earlier dithionite titration, there are no features from the difference spectra (reduced minus oxidized) characteristic of the EH_2 forms of GR or Npx (*1*). The difference spectra for the second phase reveal a small increase in A_{452} with enhanced resolution of the 478 nm shoulder as well as a continuing increase in long-wavelength absorbance centered at about 530 nm. For the most part, there are no absorbance changes beyond 650 nm in this phase, thus distinguishing the long-wavelength characteristics of the two sets of difference spectra.

With regard to the fate of the pyridine nucleotide being added during the titration, the plots of ΔA_{452} and ΔA_{350} versus equivalents of NADPH per FAD indicate nearly quantitative NADPH oxidation through 0.78 mol/FAD. It is equally clear from the linear increase in A_{350} observed beyond 1.76 equiv of NADPH added that this is most likely free NADPH, and there are no associated changes in enzyme absorbance over the range 400−800 nm. From 0.98 to 1.56 equiv of pyridine nucleotide added, however, there is an intermediate increase in A_{350} which is commensurate with the second phase of the CoADR titration, i.e., increases at 452 and 530 nm. While the A_{530} increase could be attributed to either EH_2-like Cys43-$S^- \rightarrow$ FAD or bound NADPH $\rightarrow$ FAD charge-transfer interactions involving the second active site per dimer, we really cannot distinguish between these possibilities at this point. An additional titration was performed at lower enzyme concentration so both flavin and NADPH fluorescence could be monitored (Figure 7C); these data were correlated with

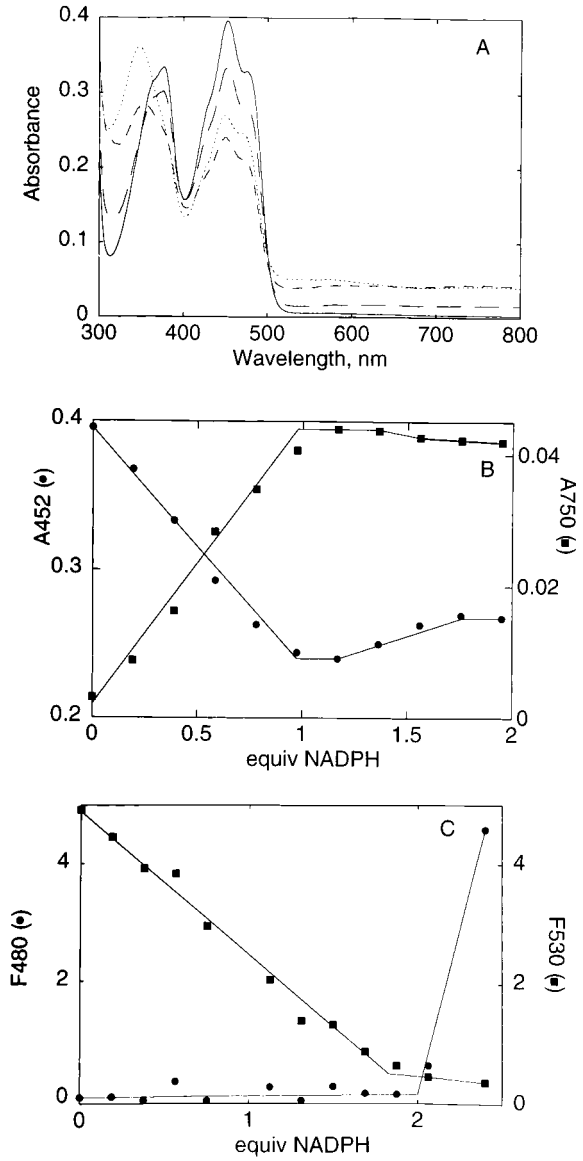

FIGURE 7: Anaerobic titration of wild-type CoADR with NADPH. (A) The 31 μM enzym e (0.75 mL) in the phosphate/EDTA buffer was reduced; spectra shown in order of increasing A_{520} correspond to oxidized enzyme (—) and enzyme after addition of 0.4 (— —), 1.2 (— —), and 1.8 (- -) equiv of NADPH/FAD. (B) Absorbance changes at 452 and 750 nm vs the number of equivalents of NADPH added. The respective end points are 0.98 and 1.76 equiv (A_{452}) and 0.98 equiv (A_{750}) of NADPH/FAD. (C) Changes in FAD (λ^{EM} = 530 nm) and NADPH (λ^{EM} = 480 nm) fluorescence vs the number of equivalents of NADPH added. These data were obtained in an experiment similar to that described in panel A, but with 10 μM CoADR. The respective end points are 1.83 equiv (F_{530}) and 2.01 equiv (F_{480}) of NADPH/FAD.

the absorbance changes at 452 nm. In this case, the end point for flavin reduction corresponded to 1.12 equiv of NADPH, and again only 1 FAD/dimer was reduced. Flavin fluorescence (λ^{EX} = 450 nm, λ^{EM} = 530 nm) decreased linearly, but at 1 equiv of NADPH/FAD, only 53% of the total quenching had occurred, consistent with the observed level of flavin reduction. The end point for the flavin fluorescence decrease (1.83 equiv of NADPH) compares very favorably to that described previously from the spectral titration (1.72−1.81 equiv at 452, 505, and 750 nm) and indicates that the addition of NADPH beyond the 1 equiv required for reduction of 1 FAD/dimer continues to lead to effective quenching of the second oxidized FAD per dimer. This could involve either reduction of the second active site to an EH_2 redox state, simple binding of NADPH at the active-site FAD, or an equilibrium distribution of these two forms. When NADPH fluorescence (λ^{EX} = 340 nm, λ^{EM} = 480 nm) is analyzed in the same experiment, the plot of F_{480} versus the number of equivalents of NADPH is essentially horizontal along the *x*-axis until a sharp increase is observed at 2.01 equiv/FAD, corresponding to free NADPH.

The combined analyses of the NADPH titration behavior for wild-type CoADR lead to the following redox scheme:

Scheme 2

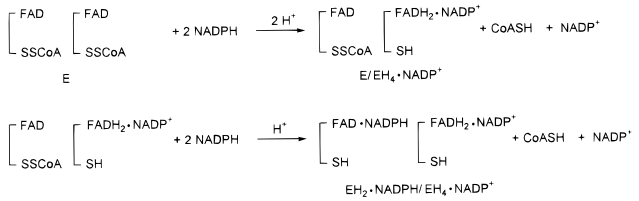

It is evident that strong active-site asymmetry is induced on interaction with NADPH, and this scheme also accounts for the reduction stoichiometry of 1 NADPH/FAD for only 50% flavin reduction (formation of $E/EH_4{\cdot}NADP^+$). We are not certain whether the values for the overall reduction stoichiometry obtained by absorbance (1.72−1.81 total equiv) and NADPH fluorescence (2.01 total equiv) are significantly different, but it is clear that the second FAD per dimer remains oxidized. Thus, it seems most likely that the asymmetric $EH_2{\cdot}NADPH/EH_4{\cdot}NADP^+$ species results on completion of the titration. Additional evidence supporting this conclusion comes from the work of delCardayré et al. (*11*), who demonstrated that aerobic incubation of 10 μM oxidized CoADR with a 20-fold excess of NADPH gave 3.0−3.2 DTNB-reactive thiols (including 1 CoASH); since there are only two half-cystines per subunit, this indicates that both Cys43-SSCoA disulfides per dimer are reduced by NADPH. A value of 2.6 reactive −SH per CoADR subunit was obtained after prior incubation with both CoAD (20-fold excess) and NADPH (2-fold excess), followed by ultrafiltration and a second incubation with NADPH (20-fold excess). In three experiments where CoADR was titrated with 1.5−2.25 equiv of NADPH/FAD, denatured anaerobically with buffered 4 M guanidine hydrochloride, and assayed with 0.1 mM DTNB, we obtained 2.6−2.8 reactive −SH/subunit. These results are in very good agreement with those of delCardayré et al. (*11*) and again support the redox sequence presented in Scheme 2.

delCardayré et al. (*11*) have also reported that CoADR is very specific for NADPH; our studies indicate that at 0.1 mM NADH the enzyme has about 17% activity relative to that of NADPH. NADH titration of wild-type CoADR exhibits a lag in ΔA_{452} equivalent to 0.9−1 mol of reductant/FAD, similar to the behavior on reduction with dithionite (but not with NADPH). The second phase continues until about 65% of the initial A_{452} is lost, but this extent of reduction is only observed in the presence of a large excess (35 equiv) of NADH. While the associated increase in A_{750} is very small, reflecting the strong preference for $NADP^+$ in formation of the charge-transfer complex with $E-FADH_2$, the level of

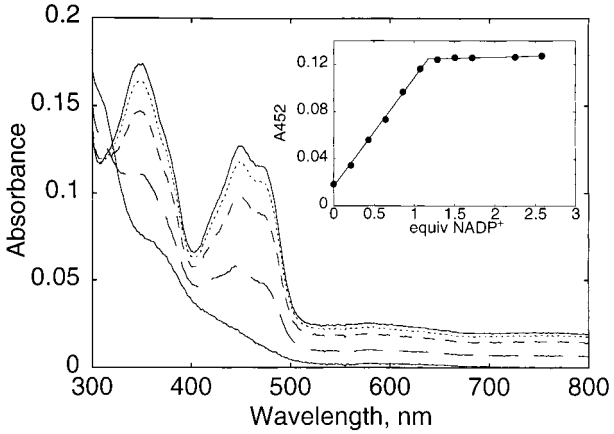

FIGURE 8: $NADP^+$ titration of the wild-type CoADR EH_4 form. The 16.1 μM CoADR (0.7 mL) was reduced in the phosphate/EDTA buffer with 2.6 equiv of dithionite/FAD, following the procedure described in the legend of Figure 4. Spectra shown, in order of increasing A_{452}, correspond to the EH_4 form (—) and enzyme after addition of 0.43 (— —), 0.86 (— —), 1.08 (- -), and 1.51 (—) equiv of $NADP^+$/FAD. In the inset is depicted the absorbance change at 452 nm vs the number of equivalents of $NADP^+$ added. The end point corresponds to 1.17 equiv of $NADP^+$/FAD.

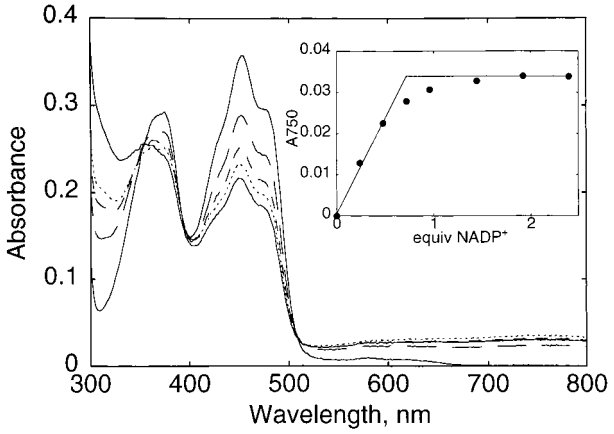

FIGURE 9: $NADP^+$ titration of the wild-type CoADR EH_2 form. The 30.5 μM CoADR (0.7 mL) in the phosphate/EDTA buffer was reduced with 1.08 equiv of dithionite/FAD, as described in the legend of Figure 4. Spectra shown, in order of decreasing A_{452}, correspond to EH_2 (—) and EH_2 after the addition of 0.48 (— —), 0.96 (— —), 1.92 (- -), and 21.4 (—) equiv of $NADP^+$/FAD. In the inset is depicted the absorbance change at 750 nm vs the number of equivalents of $NADP^+$ added. The end point corresponds to 0.71 equiv of $NADP^+$/FAD.

neutral semiquinone observed is comparable to that seen in the dithionite titration.

$NADP^+$ Titrations of CoADR EH_2 and EH_4 Forms. Consistent with the redox asymmetry exhibited by wild-type CoADR in the presence of NADPH, $NADP^+$ titration of the dithionite-reduced (EH_4) enzyme (Figure 8) leads to reoxidation of 1 FAD/dimer (ΔA_{max} = 452 nm), formation of NADPH (ΔA_{max} = 350 nm), and the appearance of the broad long-wavelength absorbance band (520−800 nm) which is characteristic of the EH_2·NADPH/EH_4·$NADP^+$ complex described above. It should be emphasized, on the basis of the nearly isosbestic behavior at 320 nm, that there is no evidence for the formation of any $NADP^+$-sulfite adduct in the course of this titration. The active-site asymmetry observed in this experiment is very reminiscent of that recently reported during NAD^+ titration of the wild-type Nox EH_2'/EH_4 form (*3*); 1 $FADH_2$/dimer formed the stable charge-transfer complex with NAD^+, while the second $FADH_2$ transferred its electrons to the remaining Cys42-SOH redox center. For the $NADP^+$ titration whose results are depicted in Figure 8, plots of ΔA versus the number of equivalents of $NADP^+$ per $FADH_2$ indicate the stoichiometric conversions of EH_4 → EH_2·NADPH and of EH_4 → EH_4·$NADP^+$, by 1.17−1.18 equiv of $NADP^+$/$FADH_2$ for observations at 452 and 750 nm, respectively. For the 2 $FADH_2$/dimer then, 2 $NADP^+$ bind to give the respective redox forms characteristic of the active-site asymmetry in CoADR.

We also examined the effect of $NADP^+$ on the EH_2 form of wild-type CoADR. The oxidized enzyme was first reduced with 1 equiv of dithionite; the dithionite syringe was then exchanged for one containing anaerobic $NADP^+$ as in the previous experiment. As shown in Figure 9, the subsequent addition of $NADP^+$ has a dramatic effect on the absorbance spectrum; these changes indicate that $NADP^+$ stabilizes an EH_2 microform (EH_2') in which the flavin of one subunit is reduced (by Cys43-SH). The A_{452} decrease observed is equivalent to an overall 45% reduction relative to the starting oxidized enzyme, and the broad long-wavelength absorbance band from 510 to 800 nm which appears, commensurate with flavin reduction, is attributed to the resulting E−$FADH_2$·$NADP^+$ complex. The spectral course of the titration is isosbestic at 349, 393, and 508 nm, and a plot of ΔA_{750} versus the number of equivalents of $NADP^+$ per FAD is consistent with a binding stoichiometry of 0.7 $NADP^+$ per EH_2 → EH_2' conversion. Still only one subunit per dimer is affected, leading to the following scheme for $NADP^+$ binding to the CoADR EH_2 form:

Scheme 3

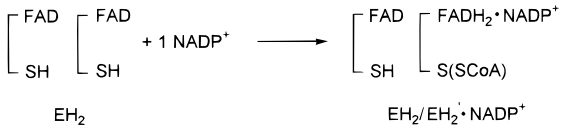

Since 1 equiv of CoASH/FAD remains in solution from the original dithionite reduction, it seems most likely that the Cys43-SSCoA mixed disulfide is the stable oxidation product of Cys43 in this anaerobic titration.

Ferricyanide Titration of NADPH-Reduced CoADR. Ferricyanide [$Fe(CN)_6^{3-}$] is an obligate one-electron acceptor with a high redox potential (E'° = +360 mV; *17*); it reacts rapidly (and stoichiometrically) with reduced flavins and reduced flavoprotein·NAD(P)H complexes (*22*). With the Npx EH_2·NADH complex, for example, ferricyanide quantitatively oxidizes the bound NADH but does not oxidize EH_2 → E (Cys42-S^- → Cys42-SOH).[3] Since we have concluded that NADPH reduction of wild-type CoADR generates 1 Cys43-SH/FAD in forming the EH_2·NADPH/EH_4·$NADP^+$ complex, we decided that ferricyanide titration of this enzyme form would provide an independent test of the redox scheme proposed for the asymmetric dimer. Figure 10A gives the spectral course for such an anaerobic experi-

[3] D. Parsonage, H. van den Burg, and A. Claiborne, unpublished results.

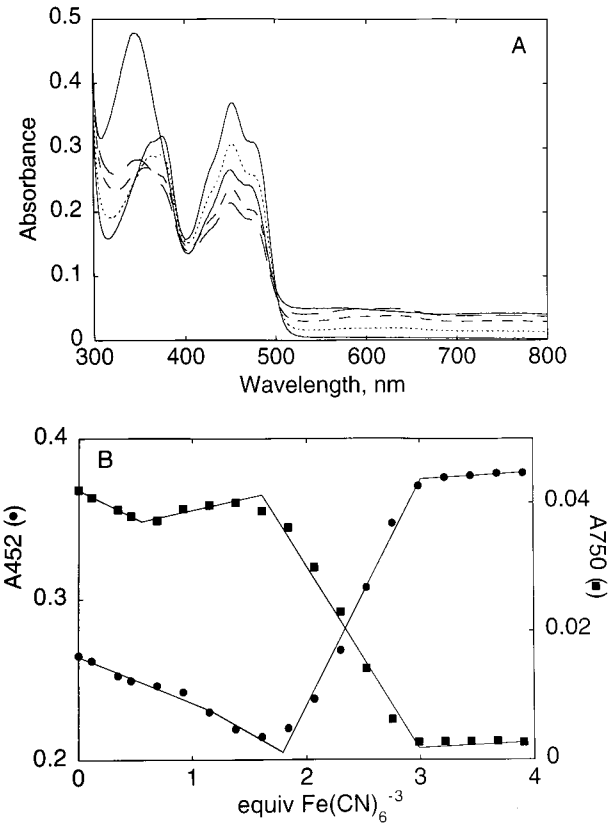

FIGURE 10: Ferricyanide titration of the wild-type CoADR EH_2·NADPH/EH_4·$NADP^+$ form. (A) The 31 μM CoADR (0.75 mL) in the phosphate/EDTA buffer was reduced with 2.34 equiv of NADPH/FAD. After the NADPH syringe was exchanged for one containing 2 mM $Fe(CN)_6^{3-}$, the titration was continued; spectra shown, in order of decreasing A_{340}, correspond to reduced enzyme (—) and enzyme after addition of 1.61 (— —), 2.07 (– –), 2.53 (- -), and 2.99 (—) equiv of $Fe(CN)_6^{3-}$/FAD. (B) Absorbance changes at 452 and 750 nm vs the number of equivalents of $Fe(CN)_6^{3-}$ added. The respective end points are 1.85 and 3.01 equiv (A_{452}) and 0.55, 1.7, and 2.99 equiv (A_{750}) of $Fe(CN)_6^{3-}$/FAD.

ment in which the CoADR sample was first reduced with 2.34 equiv of NADPH/FAD. Scheme 2 indicates that the distribution of redox components resulting at equilibrium should include 1 Cys43-SH/FAD, 0.5 $FADH_2$/FAD, 0.5 bound NADPH/FAD, and 0.34 free NADPH/FAD (0.84 total equiv of NADPH/FAD). Since Cys43-SH is not expected to react with ferricyanide, this distribution suggests that the oxidative titration should require $(0.5 + 0.5 + 0.34) \times 2 = 2.68$ equiv of ferricyanide/FAD. Through analysis of the individual absorbance spectra during this titration at wavelengths of 452, 750, 505, and 530 nm, it is clear that three distinct phases are present (Figure 10B). Difference spectra (oxidized minus reduced) for the first phase indicate a sharp decrease in A_{345} attributed to NADPH oxidation, and the plot of A_{350} versus the number of equivalents of $Fe(CN)_6^{3-}$ is linear through 0.65 mol/FAD. A small amount of neutral flavin semiquinone also appears in this phase, and plots at 505 and 530 nm (not shown) give end points of 0.7 and 0.79 mol/FAD, respectively. For the three wavelengths, the average equivalence point for the first phase is 0.71 mol of $Fe(CN)_6^{3-}$/FAD, which corresponds to 0.36 mol of NADPH (vs 0.34 mol of free NADPH as indicated by Scheme 2). We conclude that this first stage of the ferricyanide titration leads predominantly to oxidation of free NADPH.

Difference spectra for the second phase show a continuing, but more gradual, decrease in A_{345} combined with a decrease in A_{452} which continues almost linearly from the start of the titration. Sharp absorbance decreases are now seen between 500 and 675 nm, and plots at 505 and 530 nm give overall equivalence points of 1.9 and 1.87 equiv of $Fe(CN)_6^{3-}$/FAD, which compare favorably to the values of 1.85 and 1.7 equiv determined at 452 and 750 nm, respectively (Figure 10B). For the four wavelengths, the average equivalence point is 1.83 mol of $Fe(CN)_6^{3-}$/FAD, which corresponds to $(1.83 - 0.71 = 1.12)/2 = 0.56$ mol of NADPH (vs 0.5 mol of bound NADPH as indicated by Scheme 2). We conclude that the second stage of the ferricyanide titration leads predominantly to oxidation of bound NADPH:

Scheme 4

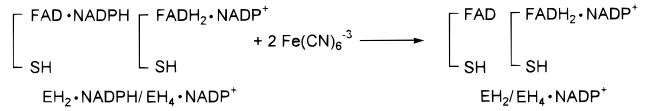

For the third phase, the difference spectra are primarily indicative of $FADH_2$ oxidation; this is seen not only in the increase in A_{452} but by the commensurate decrease in long-wavelength absorbance from 510 to 800 nm, which is due to the loss of the E—$FADH_2$·$NADP^+$ charge-transfer complex. Plots at 452 and 750 nm (Figure 10B) indicate that 1.14—1.19 equiv of $Fe(CN)_6^{3-}$/FAD is required in this final stage of the titration; the average value from plots at four wavelengths is 1.1 mol/FAD, which corresponds to 0.55 mol of $FADH_2$ (vs 0.5 mol of $FADH_2$ as indicated by Scheme 2). We conclude that the third stage of the ferricyanide titration leads predominantly to oxidation of $FADH_2$:

Scheme 5

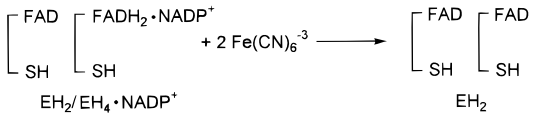

The overall stoichiometry of 2.93 equiv of $Fe(CN)_6^{3-}$/FAD compares favorably with the predicted value of 2.68 equiv/FAD, confirming that Cys43-SH in the reduced CoADR is not oxidized by $Fe(CN)_6^{3-}$. In addition, the ferricyanide titration accounts for 1.47 equiv/FAD of the NADPH in the original reduction, which gives a value of $(2.34 - 1.47) = 0.87$ Cys43-SH/FAD remaining at the end of the oxidative titration. In conclusion, this analysis corroborates the EH_2·NADPH/EH_4·$NADP^+$ redox distribution given in Scheme 2.

CoAD Titration of NADPH-Reduced CoADR. In contrast to the ferricyanide titration described above, we expected facile oxidation of Cys43-SH by CoAD, leading to the Cys43-SSCoA mixed disulfide and CoASH. Coupled with our determination that K_m(CoAD) is 3 μM, this suggested that titration of NADPH-reduced CoADR with CoAD might yield an independent determination of the redox stoichiometry and might further test the description given in Scheme 2. The enzyme was first reduced with 2.59 equiv of NADPH, giving the same distribution of redox components as described for the ferricyanide titration, but with 0.59 equiv of free NADPH/FAD. The NADPH syringe was then

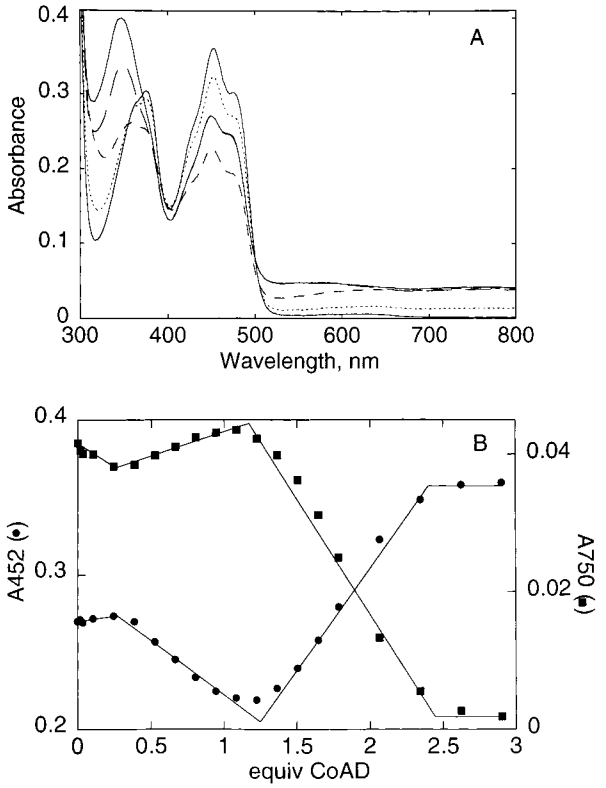

FIGURE 11: CoAD titration of the wild-type CoADR EH_2·NADPH/EH_4·$NADP^+$ form. (A) The 30.9 μM CoADR (0.86 mL) in the phosphate/EDTA buffer was reduced with 2.59 equiv of NADPH/FAD, as described in the legend of Figure 10. Spectra shown, in order of decreasing A_{350}, correspond to the reduced enzyme (—) and enzyme after addition of 0.39 (— —), 1.37 (— —), 2.07 (- -), and 3.19 (—) equiv of CoAD/FAD. (B) Absorbance changes at 452 and 750 nm vs the number of equivalents of CoAD added. The respective end points correspond to 0.27, 1.25, and 2.4 equiv (A_{452}) and 0.26, 1.17, and 2.45 equiv (A_{750}) of CoAD/FAD.

exchanged for one containing a standardized anaerobic solution of CoAD (ϵ_{260} = 33.6 mM^{-1} cm^{-1}; *11*). As in the ferricyanide titration, oxidation by CoAD proceeds in three phases (Figure 11A); the first consists of a sharp decrease in A_{340} with essentially no change in enzyme absorbance from 400 to 800 nm. The plot of A_{350} versus the number of equivalents of CoAD per FAD (data not shown) is linear through 0.48 mol, and the lags and/or small changes for the first phase as observed at 452, 750, and 580 nm give an average equivalence point of 0.29 mol of CoAD (vs 0.59 mol of free NADPH calculated to be present). As with the ferricyanide titration, the first phase corresponds primarily to the oxidation of excess NADPH; however, no flavin semiquinone appears since CoAD is a two-electron acceptor.

Phase 2 of the CoAD titration is characterized by isosbestic points at 380, 413, and 645 nm; the major absorbance changes include a continuing decrease at 343 nm as well as a decrease in enzyme absorbance with minima in the difference spectrum (oxidized minus reduced) at 450, 472, and 520 nm. There is also a small but significant increase in A_{750}. Plots at 452, 505, and 580 nm give an average overall end point of 1.22 equiv of CoAD through the second phase (Figure 11B); when corrected for the 0.29 equiv of CoAD consumed in the first phase, this corresponds to a stoichiometry of 0.93 equiv of CoAD/FAD in this stage. We conclude that the second stage of the CoAD titration leads to the preferential oxidation of the EH_2·NADPH subunit; both the bound NADPH and Cys43-SH are oxidized in this process:

Scheme 6

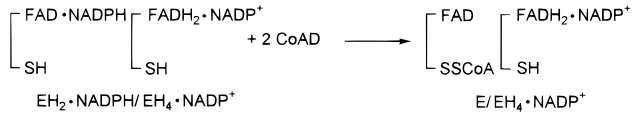

Three CoASH and one $NADP^+$ are formed in the overall reaction, which differs from the second phase of the ferricyanide titration in the fact that Cys43-SH is reactive only with CoAD.

The difference spectra for the third phase are isosbestic at 352, 400, and 505 nm; the continuing decrease at 338 nm is predominantly due to oxidation of E−$FADH_2$, as is also indicated by both the increase in absorbance at 452 and 485 nm and the loss of essentially all charge-transfer absorbance beyond 505 nm. Plots at 452, 750, and 580 nm give an average stoichiometry of 1.19 equiv of CoAD/FAD for this stage of the titration (Figure 11B), which compares favorably with the value of 1 equiv as expected on the basis of Scheme 2. We conclude that the third phase of the CoAD titration corresponds to oxidation of the remaining EH_4·$NADP^+$ subunit; both E−$FADH_2$ and Cys43-SH are oxidized in the process:

Scheme 7

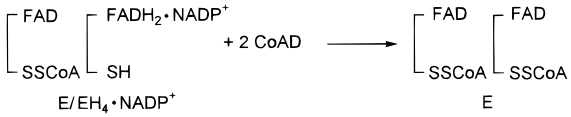

As in the previous stage, three CoASH and one $NADP^+$ result from the overall reaction, and the difference in stoichiometries (converted to 2-electron equiv) for this phase in the ferricyanide and CoAD titrations is again due to the selective reaction of Cys43-SH with CoAD.

At pH 7.0 and 25 °C, k_{cat}/K_m(CoAD) = 9 × 10^6 M^{-1} s^{-1} for wild-type CoADR, on the basis of our unpublished steady-state data.[2] Our ESI-MS and activity results for the C43S mutant suggest that the rate of the CoAD reaction with NADPH-reduced C43S CoADR should be diminished dramatically. When 60 μM CoAD was mixed anaerobically with 24 μM C43S E−$FADH_2$·$NADP^+$ enzyme, a very slow reoxidation was observed spectrally at 25 °C which corresponded to an apparent first-order rate constant of 0.024 min^{-1}; this gives a calculated second-order rate constant of 10 M^{-1} s^{-1} for the reduced mutant reaction with CoAD. This result confirms the essential role of Cys43-SH in wild-type CoADR for reduction of the disulfide substrate.

DISCUSSION

In 1977, Setlow and Setlow (*23*) reported that CoASH was the predominant low-molecular weight thiol in *B. megaterium*; concentrations of GSH plus GSSG and Cys plus cystine were <1% of that of the total CoASH plus CoAD concentration, and it was suggested that CoASH might fulfill the role served by GSH in other bacteria. In 1996, Newton

et al. (*24*) demonstrated that CoASH and Cys were the major thiols in at least one strain of *S. aureus*, while GSH was undetectable; this observation led to the suggestion (*11*) that CoASH and CoAD might function in this important human pathogen as the primary intracellular thiol/disulfide redox system. Given the calculated intracellular CoASH concentration of about 0.3 mM and the high CoASH/CoAD ratio of about 450, delCardayré et al. (*11*) proceeded to purify and characterize the NADPH-dependent flavoprotein CoADR. Along with their steady-state kinetic analyses, which demonstrated that CoADR was active with CoAD and other disulfide substrates containing at least one 4′-phosphopantetheine moiety, the enzyme was also shown to contain one NADPH-reducible protein-SSCoA disulfide in addition to one FAD per subunit. The CoADR sequence (*12*) revealed the presence of only two Cys residues, one of which (Cys43) is found within an SFXXC active-site motif also present in Nox and Npx (*6*); on this basis, it was proposed that Cys43-SH was the essential nucleophile in the reaction of reduced CoADR with CoAD, and that the oxidized form of Cys43 in the enzyme as purified was the redox-active Cys43-SSCoA disulfide. The proposal of such a mixed disulfide redox center for this flavoprotein disulfide reductase, together with the mechanism indicated for thiol/disulfide interchange involving but one active-site Cys (*11*), represents a sharp divergence from the structure−function pattern established by GR, LipDH, and other classical family members (*1*).

The combined results from activity assays, ESI-MS analyses (Figure 2), and reductive titrations with both dithionite (Figure 4) and NADPH (Figure 7) fully support the structure of the non-flavin redox center as proposed by delCardayré et al. (*11*). The C43S mutant has only about 0.03% activity, relative to that of the wild-type enzyme, in the standard spectrophotometric assay. Furthermore, the very slow rate of reoxidation ($k \sim 10$ M^{-1} s^{-1} at 25 °C) observed directly when the mutant E−$FADH_2$·$NADP^+$ complex is incubated with excess CoAD confirms that replacement of Cys43 results in an enzyme form which is essentially inactive toward the disulfide substrate, consistent with the very poor activity determined under steady-state conditions. Both measurements are also consistent with the stoichiometric reductions of the mutant CoADR observed with dithionite (1.1 equiv/FAD; Figure 3) and NADPH (1.15 equiv/FAD; Figure 5); in the latter case, the corresponding E−$FADH_2$·$NADP^+$ charge-transfer complex results, and the K_d for bound $NADP^+$ is ≤ 1 μM (Figure 6). The behavior of the CoADR C43S mutant in these reductive titrations closely parallels that of the *E. faecalis* Nox C42S mutant (*2*, *3*); the stable E−$FADH_2$·NAD^+ complex results upon NADH titration in the latter case, with a similar long-wavelength band centered at 725 nm. The stoichiometric reductions observed with the respective mutant enzymes demonstrate that Cys mutagenesis eliminates the non-flavin redox center in each case: Cys43-SSCoA in CoADR and Cys42-SOH in Nox. Further direct evidence for the Cys43-SSCoA disulfide in wild-type CoADR comes from the ESI-MS analysis of the recombinant enzyme. Initially, we were concerned about whether the recombinant enzyme as purified would yield 100% of the CoASH-modified Cys43 form, although the DTNB and thiol analyses reported by delCardayré et al. for CoADR purified from *S. aureus* were duplicated with the enzyme purified from *E. coli*.[4] Newton et al. (*24*) have shown that some *E. coli* strains have intracellular CoASH concentrations as high as 0.15 mM; the strong preference exhibited by Cys43-SH (*11*) in reacting with the CoASH moieties of mixed disulfide substrates (e.g., CoASSG), combined with the failure to react with GSSG or cystine, accounts for the fact that Cys43 is fully modified by CoASH whether the enzyme is purified from *S. aureus* or recombinant *E. coli*. The C43S mutant gives a single-component spectrum on ESI-MS analysis corresponding to the calculated (minus CoASH) *m* value of 49 143 Da (Figure 2), proving that Cys43 is the CoASH attachment site.

Although a detailed kinetic analysis for CoADR will be presented in a separate communication, it is important to point out that the specific activity and k_{cat} (27 s^{-1}) values determined in this laboratory, using a standard spectrophotometric assay at 25 °C based on NADPH oxidation, differ significantly from the k_{cat} value of 1000 s^{-1} reported for the enzyme at 37 °C (*11*). We have not undertaken any study of the temperature dependence for this reaction, but to account for the two observed k_{cat} values using only the temperature difference would require an Arrhenius energy of activation of 55 kcal/mol, in dramatic contrast to the usual value of 10−11 kcal/mol for enzyme-catalyzed reactions (*25*). Another concern with regard to the previously reported value for k_{cat} is that a turnover number of 1000 s^{-1}, given the published K_m(NADPH) and K_m(CoAD) values of 1.6 and 11 μM, respectively, yields k_{cat}/K_m constants of 6×10^8 and 9×10^7 M^{-1} s^{-1}, respectively. Both values approach or exceed the generally accepted limiting rate constant for a diffusion-controlled enzyme−substrate encounter of 10^8−10^9 M^{-1} s^{-1} (*25*−*27*). At 25 °C, the k_{cat}/K_m(CoAD) value of 9×10^6 M^{-1} s^{-1}, as determined in this laboratory, compares quite favorably to the values reported for *E. coli* GR (4×10^6 M^{-1} s^{-1} with GSSG at 30 °C; *28*) and *Crithidia fasciculata* trypanothione reductase (10^7 M^{-1} s^{-1} with trypanothione at 27 °C; *29*); the kinetic data available for LipDH (*30*), pantethine 4′,4″-diphosphate reductase (*9*), and coenzyme M-disulfide reductase (*10*) give specificity constants of $3-15 \times 10^4$ M^{-1} s^{-1} with the respective disulfide substrates over a range of temperatures. Given that CoAD is a rather complex substrate molecule ($m = 1533$ Da), we find it quite interesting (*25*) that CoADR is still capable of supporting an encounter rate constant of 10^7 M^{-1} s^{-1}.

Dithionite titration of wild-type CoADR is fully consistent with the presence of one FAD and one Cys43-SSCoA redox center per subunit (Figure 4), and there appears to be a significant separation in $E'°$ values for the disulfide and FAD based on the clear lag in the A_{452} change during the titration. Still it is surprising that the EH_2 form of CoADR generated with 1 equiv of dithionite gives no spectral evidence for Cys43-S^- → FAD charge-transfer interaction. The EH_2 forms of both Nox and Npx exhibit this spectral feature (*3*, *18*), centered at about 530 nm, which requires the thiolate form of the charge-transfer Cys as well as proper orientation of the thiolate → FAD donor/acceptor pair. We have shown, for example, that an R303M mutant of Npx with a pK_a of ~8 for the EH_2 Cys42-SH has negligible charge-transfer absorbance at pH 7.0 (*31*). Given the quantitative oxidation observed for NADPH-reduced CoADR with substoichiometric aliquots of CoAD at pH 7.0 (Figure 11), we prefer to

[4] S. delCardayré, personal communication.

conclude that the pK_a for Cys43-SH is comparable to the values for the charge-transfer thiols in Npx, GR, and LipDH, i.e., $\leq$4.8 (*1*). A key mechanistic contrast between Npx and Nox and the classical disulfide reductases is that the single active-site Cys42 serves as both the charge-transfer donor to FAD and the active-site nucleophile toward R-OOH (R = H or FADH; *2*, *20*); there is no distinct interchange thiol, but the electrophilic peroxide is either H_2O_2 (a small, neutral substrate) or an FAD C(4a)-hydroperoxide poised for reaction with Cys42-S^- within the active site. With CoADR the oxidizing substrate is a large, charged molecule which may not easily access the active-site Cys43-S^- if it is engaged as a charge-transfer donor to the FAD. Thus, we envisage a somewhat more flexible orientation for the Cys43-thiolate in CoADR, depending on the redox state. In the oxidized enzyme, the Cys43-SSCoA disulfide must (presumably) be oriented to receive electrons via the flavin, but in the EH_2 form, the nascent Cys43-thiolate must be able to access and reduce the disulfide bond of CoAD. Despite the absence of significant charge-transfer character in EH_2, the fluorescence of oxidized CoADR is quenched by about 90% in this intermediate (Figure 4). While we presently interpret this result in terms of an effect of the nascent Cys43-thiolate, it is also important to compare these results with the behavior of the *E. coli* LipDH (*32*). In the latter case, reduction with 1 equiv of dithionite led to a mixture of three different electronic forms of EH_2: (1) a fluorescent species [FAD, $(-SH)_2$] which is about 25% as fluorescent as E at pH 7.1, (2) a nonfluorescent charge-transfer species [FAD, $(-SH)_2$] comparable to that seen in GR, and (3) a species with reduced flavin characteristics [$FADH_2$, (-SS-)]. The fluorescent [FAD $(SH)_2$] form does not exhibit charge-transfer absorbance, and Wilkinson and Williams (*32*) also showed that as the pH was increased over the range of 5.8−8.0, the equilibrium distribution shifted in favor of the charge-transfer species, with a concomitant loss of fluorescence. Still, even at pH 7.1, 52% of the LipDH EH_2 species was present as the charge-transfer form, in sharp contrast to our results with CoADR at pH 7.0.

There is clear evidence for an equilibrium distribution within the two-electron reduced CoADR involving [FAD, (-SH)] and [$FADH_2$, (-SS-)] forms; the distribution shifts dramatically away from the FAD species that is predominant on reduction with 1 equiv of dithionite (Figure 4) toward the $FADH_2$ form in the presence of $NADP^+$ (Figure 9). $NADP^+$ binds tightly, giving rise to the $FADH_2$·$NADP^+$ charge-transfer complex, and the marked decrease in A_{452} which is concomitant with formation of this complex reflects intramolecular electron transfer from Cys43-SH to FAD. Still, only about one-half of the flavin is reduced at saturating $NADP^+$ concentrations; this is only one manifestation of the active-site asymmetry for CoADR that will be discussed subsequently. Thinking that the residual fluorescence observed with the CoADR EH_2 intermediate might specifically reflect the FAD species, we also followed this property during the $NADP^+$ titration, anticipating a decrease on conversion of FAD $\rightarrow$ $FADH_2$. However, there was no clear change in flavin fluorescence commensurate with the change in the absorption spectrum. A careful study of the pH dependence of these spectroscopic properties will be required to further define this apparent equilibrium of EH_2 species.

Given the pronounced effect of $NADP^+$ on the dithionite-generated EH_2 intermediate, it is not surprising that the spectral course of the NADPH titration (Figure 7) is quite different from that with dithionite (Figure 4). Addition of 1 equiv of NADPH/FAD leads to reduction of one FAD and one Cys43-SSCoA per dimer, with no lag in ΔA_{452} as seen with dithionite. The $FADH_2$·$NADP^+$ complex which results should be formally equivalent to that appearing on $NADP^+$ titration of EH_2, but a close inspection of Schemes 2 and 3 reveals an important distinction between the two proposed asymmetric dimers at this stage. While the simple and direct interpretation of the NADPH titration leads to the proposal of the E/EH_4·$NADP^+$ dimer, the $NADP^+$ titration result (Figure 9) indicates clearly that within an EH_2 monomer, the redox potential for that flavin ($FADH_2$) is shifted on $NADP^+$ binding to a new value much higher than that for its Cys43-SSCoA/Cys43-SH redox partner. $NADP^+$ is a ligand which preferentially binds $FADH_2$ and perturbs the apparent E'° for the FAD/$FADH_2$ couple (*33*), and on this same basis, it seems unlikely that NADPH titration at the 1 equiv/FAD stage would lead to Cys43-SSCoA reduction on that same $FADH_2$·$NADP^+$ subunit. Therefore, in view of the combined NADPH and $NADP^+$ titration data, we believe that the asymmetric EH_2/EH_2'·$NADP^+$ redox state is most likely to result on reduction of wild-type CoADR with 1 equiv of NADPH/FAD:

Scheme 8

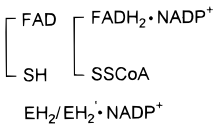

The differential behavior of the two active sites per dimer in this respect is another manifestation of the subunit asymmetry mentioned previously.

As the titration continues, NADPH binds the EH_2 subunit but does not reduce this FAD (Figure 7). Rather, NADPH binding appears to promote intramolecular electron transfer within the EH_2' subunit, leading eventually to reduction of the remaining Cys43-SSCoA redox center at the expense of NADPH with no net loss of the $FADH_2$·$NADP^+$ charge-transfer complex. The second phase of NADPH titration, therefore, leads to no change in A_{750}; the absorbance increases at 350, 452, and 530 nm reflect the equilibrium distribution on each addition of NADPH between formation of stable EH_2·NADPH subunits and NADPH-dependent conversion of EH_2'·$NADP^+$ $\rightarrow$ EH_4·$NADP^+$ subunits:

Scheme 9

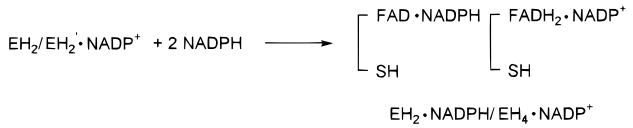

The influence of tightly bound $NADP^+$ in "directing" the flow of electrons to the two disulfide centers per dimer is entirely consistent with the observation that NADH titration, which does not yield a strong $FADH_2$·NAD^+ complex, exhibits the same lag of 1 equiv in ΔA_{452} as seen in the dithionite titration.

Titration of NADPH-reduced CoADR with CoAD, when corrected for the 0.29 equiv of CoAD consumed in oxidation

of excess NADPH, corresponds to an overall stoichiometry of 2.12 equiv/FAD (Figure 11); this result is in excellent agreement with that predicted for the EH_2·NADPH/EH_4·$NADP^+$ form of CoADR described above. In addition to confirming the quantitative results from NADPH titrations and DTNB analyses, the CoAD titration demonstrates that the asymmetric reduced CoADR dimer is capable of reducing the physiological substrate. We have already addressed the thermodynamic inequivalence of wild-type CoADR with regard to the two FADs per dimer and their respective interactions with NADPH (and of the corresponding $FADH_2$ forms with $NADP^+$); in general, our analysis of the equilibrium properties of CoADR is very reminiscent of the classical study of mercuric reductase (MR) by Miller et al. (*34*), which led to an alternating sites hypothesis for cooperativity in catalysis. While these aspects have been discussed in detail recently by us (*2*, *3*) in describing the thermodynamic and kinetic active-site inequivalence in both wild-type and C42S mutant forms of Nox, one particular point from the MR study has special relevance to the present work with CoADR. NADPH titration of the MR C135A/C140A double mutant lacking the redox-active disulfide leads to reduction of only 1 FAD/dimer; the asymmetric E·NADPH/EH'_2·$NADP^+$ complex which results is directly comparable to the EH_2·NADPH/EH_4·$NADP^+$ intermediate seen with wild-type CoADR.

Kinetic analysis of the reduced MR mutant complex reaction with O_2 led to a sequential cooperative model in which reoxidation of the $FADH_2$ subunit leads to rapid intramolecular electron transfer within the E·NADPH subunit; reaction of the resulting $FADH_2$ with O_2 accounts for nearly the entire A_{465} increase observed. While the details of such a kinetic model, as they may pertain to CoADR catalysis of disulfide reduction, await further analysis, the spectral course for the two major phases of the CoAD titration (Figure 11) is essentially the reverse of the NADPH titration itself (Figure 7). There is no loss of $FADH_2$·$NADP^+$ charge-transfer absorbance during the first phase of enzyme reoxidation (0.93 equiv of CoAD/FAD), but essentially complete oxidation of bound NADPH (EH_2·NADPH subunit) is easily measured at 343 nm. The simplest and most direct interpretation of this process involves the formation of the E/EH_4·$NADP^+$ intermediate as outlined in Schemes 6 and 7, but a thorough kinetic analysis of the oxidative half-reaction with CoAD will be necessary before any catalytic role can be ascertained for this asymmetric species.

It is important to stress that CoADR now represents a second case, to our knowledge, where a redox-active protein disulfide has been functionally replaced by a single Cys. Thus, CoADR catalyzes a reaction fundamentally similar to that of GR; Choi et al. (*35*) have recently reported the 2.0 Å crystal structure of a novel human peroxidase enzyme, hORF6, which appears to function in vivo in the reduction of peroxides. This "1-Cys peroxiredoxin" contains a single Cys-SOH derivative of Cys47, as revealed in the crystal structure; hORF6 is a homologue of the "2-Cys peroxiredoxin" AhpC component of the *Salmonella typhimurium* alkyl hydroperoxide reductase, which utilizes a redox-active intersubunit disulfide involving Cys46 and Cys165′ in the catalytic reduction of peroxide substrates (*36*, *37*). delCardayré and Davies (*12*) have correctly pointed out that CoADR is the first flavoprotein disulfide reductase shown to contain the SFXXC active-site motif present in Nox and Npx, and the *Streptococcus mutans* Nox sequence is 29% identical, overall, to that of CoADR. However, sequence alignments for the six true Nox and Npx proteins (i.e., purified and demonstrated to function catalytically in NADH-dependent reduction of either $O_2 \rightarrow 2H_2O$ or $H_2O_2 \rightarrow 2H_2O$) give the following active-site motif: ISFLXCGXXL.[5] On this basis, CoADR has only three of the seven absolutely conserved residues found in the Nox/Npx "motif", one of which is the essential Cys. Also, the *Methanococcus jannaschii* "NADH oxidase" referred to by delCardayré and Davies (*12*) does not have any form of Nox/Npx motif; it only conserves the Ile and Cys residues (*38*). In fact, if one compares the NADH oxidase sequences reported for the methanogens *M. jannaschii* and *Methanobacterium thermoautotrophicum* (*39*), the putative "active-site Cys" sequence is more indicative of yet a third distinct group of FAD enzymes related to, but distinct from, the GR and Npx/Nox groups, respectively. An alignment of the CoADR sequence with the methanogenic "Nox" consensus (AYSPCAIPYV) reveals that CoADR retains five of the ten absolutely conserved residues. So we would suggest that CoADR may be more closely related to these archaeal "Nox" homologues than to the true Nox/Npx group. The possibility that the methanobacterial coenzyme M-disulfide reductase referred to previously (*10*) corresponds to the *M. thermoautotrophicum* "Nox" is one that should be pursued vigorously.

[5] D. Parsonage, T. C. Mallett, and A. Claiborne, unpublished results.

ACKNOWLEDGMENT

We thank Dr. Steve delCardayré and Dr. Julian Davies for providing the pXCDR expression plasmid, and we also thank Dr. delCardayré for critical reading of the manuscript. We thank Dr. Derek Parsonage for assistance in the initial phase of this work and for providing the sequence alignments, and we thank Dr. Mike Thomas and Mr. Mike Samuel for providing the mass spectrometry analyses and for helpful discussions.

REFERENCES

1. Williams, C. H., Jr. (1992) in *Chemistry and Biochemistry of Flavoenzymes* (Müller, F., Ed.) Vol. III, pp 121−211, CRC Press, Boca Raton, FL.
2. Mallett, T. C., and Claiborne, A. (1998) *Biochemistry 37*, 8790−8802.
3. Mallett, T. C., Parsonage, D., and Claiborne, A. (1999) *Biochemistry 38* (in press).
4. Claiborne, A., Crane, E. J., III, Parsonage, D., Yeh, J. I., Hol, W. G. J., and Vervoort, J. (1997) in *Flavins and Flavoproteins 1996* (Stevenson, K. J., Massey, V., and Williams, C. H., Jr., Eds.) pp 731−740, University of Calgary Press, Calgary, AB.
5. Yeh, J. I., Claiborne, A., and Hol, W. G. J. (1996) *Biochemistry 35*, 9951−9957.
6. Ross, R. P., and Claiborne, A. (1992) *J. Mol. Biol. 227*, 658−671.
7. Miller, H., Mande, S. S., Parsonage, D., Sarfaty, S. H., Hol, W. G. J., and Claiborne, A. (1995) *Biochemistry 34*, 5180−5190.
8. Claiborne, A., Miller, H., Parsonage, D., and Ross, R P (1993) *FASEB J. 7*, 1483−1490.
9. Swerdlow, R. D., and Setlow, P. (1983) *J. Bacteriol. 153*, 475−484.
10. Smith, S. G., and Rouviére, P. E. (1990) *J. Bacteriol. 172*, 6435−6441.

11. delCardayré, S. B., Stock, K. P., Newton, G. L., Fahey, R. C., and Davies, J. E. (1998) *J. Biol. Chem. 273*, 5744−5751.
12. delCardayré, S. B., and Davies, J. E. (1998) *J. Biol. Chem. 273*, 5752−5757.
13. Parsonage, D., Luba, J., Mallett, T. C., and Claiborne, A. (1998) *J. Biol. Chem. 273*, 23812−23822.
14. Poole, L. B., and Claiborne, A. (1988) *Biochem. Biophys. Res. Commun. 153*, 261−266.
15. Leatherbarrow, R. (1987) *Enzfitter*, Biosoft, Hills Road, Cambridge, U.K.
16. Circular OR-18 (1961) P·L Biochemicals, Inc., Milwaukee, WI.
17. Loach, P. A. (1976) in *Handbook of Biochemistry and Molecular Biology* (Fasman, G. D., Ed.) 3rd ed., Vol. 1, pp 122−130, CRC Press, Boca Raton, FL.
18. Poole, L. B., and Claiborne, A. (1986) *J. Biol. Chem. 261*, 14525−14533.
19. Crane, E. J., III, Vervoort, J., and Claiborne, A. (1997) *Biochemistry 36*, 8611−8618.
20. Parsonage, D., and Claiborne, A. (1995) *Biochemistry 34*, 435−441.
21. Crane, E. J., III, Parsonage, D., and Claiborne, A. (1996) *Biochemistry 35*, 2380−2387.
22. Massey, V., Müller, F., Feldberg, R., Schuman, M., Sullivan, P. A., Howell, L. G., Mayhew, S. G., Matthews, R. G., and Foust, G. P. (1969) *J. Biol. Chem. 244*, 3999−4006.
23. Setlow, B., and Setlow, P. (1977) *J. Bacteriol. 132*, 444−452.
24. Newton, G. L., Arnold, K., Price, M. S., Sherrill, C., delCardayré, S. B., Aharonowitz, Y., Cohen, G., Davies, J., Fahey, R. C., and Davis, C. (1996) *J. Bacteriol. 178*, 1990−1995.
25. Gutfreund, H. (1972) *Enzymes: Physical Principles*, John Wiley and Sons, New York.
26. Jencks, W. P. (1969) *Catalysis in Chemistry and Enzymology*, McGraw-Hill, Inc., New York.
27. Fersht, A. (1985) *Enzyme Structure and Mechanism*, 2nd ed., W. H. Freeman and Co., New York.
28. Scrutton, N. S., Berry, A., and Perham, R. N. (1987) *Biochem. J. 245*, 875−880.
29. Shames, S. L., Fairlamb, A. H., Cerami, A., and Walsh, C. T. (1986) *Biochemistry 25*, 3519−3526.
30. Reed, J. K. (1973) *J. Biol. Chem. 248*, 4834−4839.
31. Crane, E. J., III, and Claiborne, A. (1997) in *Flavins and Flavoproteins 1996* (Stevenson, K. J., Massey, V., and Williams, C. H., Jr., Eds.) pp 773−776, University of Calgary Press, Calgary, AB.
32. Wilkinson, K. D., and Williams, C. H., Jr. (1979) *J. Biol. Chem. 254*, 852−862.
33. Clark, W. M. (1960) *Oxidation−Reduction Potentials of Organic Systems*, Williams and Wilkins Co., Baltimore, MD.
34. Miller, S. M., Massey, V., Williams, C. H., Jr., Ballou, D. P., and Walsh, C. T. (1991) *Biochemistry 30*, 2600−2612.
35. Choi, H.-J., Kang, S. W., Yang, C.-H., Ree, S.-G., and Ryu, S.-E. (1998) *Nat. Struct. Biol. 5*, 400−406.
36. Ellis, H. R., and Poole, L. B. (1997) *Biochemistry 36*, 13349−13356.
37. Ellis, H. R., and Poole, L. B. (1997) *Biochemistry 36*, 15013−15018.
38. Bult, C. J., et al. (1996) *Science 273*, 1058−1073.
39. Smith, D. R., et al. (1997) *J. Bacteriol. 179*, 7135−7155.

BI9825899